

On the different role of protons and neutrons in antinucleon annihilations on nuclei.

A. Bianconi ^a, G. Bonomi ^a, M.P. Bussa ^a, G. Gomez ^a,
 E. Lodi Rizzini ^a, L. Venturelli ^a, A. Zenoni ^a,

^a*Dip. di Chimica e Fisica per l'Ingegneria e per i Materiali, Università di Brescia
 and INFN, Sez. di Pavia, Italy*

Abstract

We compare data of antineutron and antiproton annihilation cross sections on different targets at very low energies. After subtracting Coulomb effects, we observe that the ratio between the $\bar{n}p$ and $\bar{p}p$ annihilation cross sections is an oscillating function of the energy at momenta smaller 300 MeV/c. This nontrivial behavior is confirmed by the analysis of the relative number of $\bar{p}n$ and $\bar{p}p$ annihilations in nuclei. We show that a part of the strong shadowing phenomena in \bar{p} -nucleus annihilations can be explained in terms of this oscillation, while a part requires different explanations.

1 Introduction.

Recently data on $\bar{n}p$ annihilation in the range 40-400 MeV/c (for the laboratory \bar{n} momentum k) have been produced by the Obelix Collaboration[1]. We would like to compare these with other data on $\bar{p}p$ and \bar{N} -nucleus annihilation. In particular, we are interested in: \bar{n} annihilation on nuclei from ^{12}C to ^{207}Pb in the range 180-280 MeV/c[2]; $\bar{p}p$ annihilation from 30 to 180 MeV/c[3]; $\bar{p}D$, $\bar{p}^4\text{He}$ and $\bar{p}^{20}\text{Ne}$ at small momenta, down to 45 MeV/c[5,6]; \bar{p} -nucleus annihilation on intermediate nuclei at larger momenta (over 200 MeV/c, see[7] for a recollection of these data); and on the ratio between $\bar{p}p$ and $\bar{p}n$ annihilations inside nuclear targets[8]. We will start by comparing $\bar{p}p$ and $\bar{n}p$ data, and then we will try to correlate these with the low energy nuclear data.

One of our aims is simply to compare $\bar{n}p$ and $\bar{p}p$ annihilation cross sections. This comparison is a delicate operation, because it requires subtraction of Coulomb effects, and comparison of data coming from different experiments with antiproton and antineutron beams. Due to the difficulties in calculating a

100 % reliable flux normalization, it is preferable, as far as possible, to compare data from the same experiment.

A second goal of this work is to establish which is the degree of correlation between antineutron-nucleon and antinucleon-nucleus data. Indeed, as better discussed later, $\bar{p}p$ data below 600 MeV/c can be well fitted via energy independent optical potentials, while $\bar{n}p$ data show a nontrivial energy dependence that should be reflected in the energy dependence of nuclear annihilations.

Another interesting point is the role of the different isospin channels in the low energy nuclear shadowing. It has been demonstrated that a marked nuclear shadowing characterizes low energy \bar{N} -nucleus annihilation cross sections[5,9–19]. For this phenomenon it is possible to imagine two classes of explanations. First, general quantum mechanical processes, as described in a later section. Mechanisms of this kind do not discriminate too much between different annihilation channels. On the other side we may imagine a role for peculiar properties of single nuclear species. Indeed, the data are rather incomplete and impossible to organize in a systematic way. In particular a different N/Z composition, or a different N/Z distribution near the nuclear surface can be relevant, since most of the theoretical models (for reviews see e.g. [20–26]) establish peculiar properties for the different isospin channels, properties which are normally derived either from G-parity (or C-parity[27]) transformations of the better known nucleon-nucleon potentials, or from peculiar quark diagrams. So, to summarize this point, it is relevant to establish how much of the low energy nuclear shadowing of annihilation processes can be due to general mechanisms, and how much is due to the nuclear composition in terms of protons and neutrons, and to the details of the nuclear structure.

We limit ourselves to a phenomenological analysis of the data, with standard methods of nuclear physics, without entering the debate about the underlying hadronic structure mechanisms governing the annihilation process. Of course, it is not always possible to separate completely the two levels of the analysis, i.e. nuclear and hadronic. Wide reviews on the debate concerning the annihilation mechanisms can be found in the references listed above. Experimental (scattering and annihilation) data up to 1994 are recollected in [7], data on antiprotonic atoms up to 1988 in [28], and a very recent account of the many problems related with the antinucleon experimental techniques can be found in [29].

We still lack a well founded method that can be properly used at low energies to link the shadowing properties (that automatically arise from an optical potential treatment[13,16,15]) with the details of the nuclear structure and internal motions (which are taken into account in Impulse Approximation inspired treatments). The main exception in this respect is Deuteron, which has been considered by some authors[11,12,15] and where it was possible to

relate clearly the overall antinucleon-nucleus processes with the antinucleon-nucleon interactions. With more complex nuclei, optical potential analyses have been carried on to study antiprotonic atoms[30–35]. At momenta over 200 MeV/c the KMT method[36] has been used in [37] and the Glauber method[38] in [39] (and probably in other works). In the present work our hope is that some interesting information can be separately extracted from a PWIA and an optical potential analysis.

For the sake of brevity we will indicate total \bar{n} and \bar{p} annihilation cross sections with TNA and TPA respectively, specifying the target. We will indicate as F_A the ratio between $\bar{p}n$ and $\bar{p}p$ annihilations in a given nucleus with atomic number A .

Concerning the choice of an optical potential for discussing nucleon-antinucleon annihilation, it is well known that many quite different optical potentials fitted successfully pre-Obelix nucleon-antinucleon data[27,40–51] and they can probably fit the data under discussion too, since these data do not represent such a strong constraint. Here and in previous papers[16–18] we have relied on very simple optical potentials, with Woods-Saxon shape, the same parameters for each spin channel and no energy dependence in the momentum range 0–600 MeV/c (more indications are given in section 3). Although such potentials cannot reproduce the full phenomenology of nucleon-antinucleon interactions, they seem sufficient for fitting the available $\bar{p}p$ low energy data. With the $\bar{n}p$ annihilation data, as described in section 3, a higher level of sophistication is perhaps necessary.

2 The role of Coulomb interactions. Apparent violation of the isospin invariance.

Comparison of annihilation data with different projectiles and targets is nonsense without subtracting Coulomb effects at momenta below 200 MeV/c. The traditional estimation[52] has undergone modifications[53,54,17] in the last years. Qualitatively the effect of the Coulomb forces is to focus the projectile wavefunction in the annihilation region, which is a spherical shell of thickness 0.5–1 fm[20,55,37] at the target proton/nucleus surface.

In a previous work[17] we gave analytical expressions for the correcting \bar{p} -nucleus enhancement factors. E.g., for the $\bar{p}p$ annihilation cross section the enhancement factor can be reproduced within 5 % in the range 30–400 MeV/c by the function $1 + 0.0003\beta^{-2}$. To calculate the enhancement factor we considered some completely different optical potentials. All of them included the electrostatic potential of a spherical charge distribution and fitted the available low energy data. Then we removed the electrostatic potential and calculated

again the annihilation rates. The obtained Coulomb enhancement factor was sufficiently independent of the choice of the strong part of the optical potential, in the considered momentum range.

An observation is necessary concerning apparent “violations” of the isospin invariance. Isospin symmetry suggests that: (i) $\bar{n}p$ cross sections are equal to $\bar{p}n$ ones; (ii) $\bar{p}p$ and $\bar{n}n$ are equal apart from electromagnetic effects; (iii) the four cross sections that one can imagine are actually combinations of two. In principle this is undoubtful, but in practice it does not work, and an example can clarify the point. Normally, $\bar{n}p$ data come from collisions between free antineutrons and protons, while $\bar{p}n$ cross sections are extracted from deuteron targets, with two consequences:

- 1) The antiproton is attracted by the deuteron charge. The range of action of the Coulomb forces is much larger than the deuteron radius, with the result that the $\bar{p}n$ annihilation rate is almost as much “Coulomb distorted” as the $\bar{p}p$ one, so it should be expected to be larger (much larger at very low energies) than the $\bar{n}p$ one. This problem is not present at momenta $>> 100$ MeV/c, where Coulomb focusing effects can be neglected.
- 2) As already noticed[5,10,13,16,14,18], below 60 MeV/c shadowing effects in nuclei are so strong that the $\bar{p}D$ annihilation cross section is smaller than the corresponding $\bar{p}p$ one in the laboratory frame, or approximately equal in the center of mass frame (due to the different transformations relating laboratory with center of mass variables for the cases of proton and deuteron targets). In both cases $\sigma_{\bar{p}D}$ is much smaller than $\sigma_{\bar{p}p} + \sigma_{\bar{n}p}$.

The previous example should clarify that, although it is very likely that one would find $\sigma_{\bar{n}p} \approx \sigma_{\bar{p}n}$ in an experiment on *free* neutrons, comparisons involving different isospin channels for $k << 100$ MeV/c should be performed with the greatest care as far as free neutron targets, or antiproton targets, are not available. One should therefore be aware that an isospin decomposition cannot be completely free from model dependence.

3 Nuclear shadowing effects.

Recent experimental data[5,10,18] show that at antinucleon momenta (in the laboratory) below 60 MeV/c the nuclear shadowing effect is very strong. Below 60 MeV/c antiproton annihilation rates on Deuteron and ${}^4\text{He}$ are smaller than on Hydrogen. The annihilation rate on ${}^{20}\text{Ne}$ is larger but not that much[6]. This and related phenomena has been discussed by us and other authors[11–14,16,19].

Rather independently of the mechanism underlying the annihilation process, it had been previously demonstrated that in the framework of the multiple scattering theory[11], of variational methods[12] and of optical potential treatments[13,16] one can predict such shadowing effects. It has been reported[13] that also in the coupled-channel approach one can obtain the same result.

The fact that different methods lead to similar results suggested us to investigate the problem from a more general and qualitative, although less precise, point of view. In our work[19] we have shown that due to the quantum uncertainty principle the \bar{n} -nucleus cross sections should be almost A -independent, apart for fluctuations due to nuclear surface effects. Consequently the \bar{p} -nucleus cross sections should depend on the target because of its electric charge only. The underlying argument is that most of the existing models (see the suggested references [20–25]) and analyses[55,37,51] establish that the annihilation process takes place when the centers of mass of the antinucleon and of the target nucleus are at a relative distance d such that $R_{nucleus} < d < R_{nucleus} + \Delta$, where $\Delta \sim 1$ fm (or smaller, depending on the model) does not depend too much on the target. So the annihilation is equivalent to a measurement of the projectile-target relative distance with uncertainty $\Delta < 1$ fm, and this measurement is incompatible with a relative momentum $\ll 200$ MeV/c.

To see it another way, we distinguish between two classes of nuclear reactions. On one side, inelastic reactions where the entire nucleus is involved, as in compound nucleus reactions, but the underlying projectile-nucleon processes are elastic (e.g. neutron induced nuclear reactions). In this case the characteristic reaction region coincides approximately with the target nucleus. Then the uncertainty Δ coincides approximately with the nuclear radius. On the other side, we find reactions where a strong inelasticity is present at the projectile-nucleon level. In this case reactions deep inside the nuclear volume are rare, the reaction region is a shell at the surface of the target nucleus, with thickness Δ , and Δ is approximately the same for all the possible targets.

The consequence of the limitations imposed by the uncertainty principle is that for antinucleon momenta $k \ll 1/\Delta$ the total reaction cross section becomes much smaller than its possible unitarity limit. This is also established by the well known[52] low energy limit for the phase shifts: $\delta_l \propto k^{2l+1}$ for $k \rightarrow 0$. The unitarity limit is reached when a partial wave is completely absorbed in the reaction process, which means $\exp(i\delta_l) = 0$, i.e. $Im(\delta_l) = \infty$, so the unitarity limit cannot be attained at small enough k . Uncertainty considerations suggest that for $k \gg 1/\Delta$ it is possible, for strong enough reactions, to saturate the unitarity limit, while for $k \ll 1/\Delta$ we are in the situation where $\delta_l = O(k^{2l+1})$, whatever the strength of the reaction. A paradoxical consequence is that a smaller Δ corresponds to what would be a stronger reaction at large energies, so that at low energies “stronger” interactions can lead to a smaller reaction rate. This fact can be verified in optical potential treatments.

On the ground that the projectile wavefunction Ψ is completely damped within a range Δ (i.e. $|\Psi|$ is large for $r > R_{nucleus} + \Delta$ and very small for $r < R_{nucleus}$) it is straightforward to demonstrate that for the scattering length α we have (approximately):

$$Im(\alpha) \approx -\Delta,$$

$$Re(\alpha) \approx +R_{nucleus}.$$

Indeed, the Ψ damping requirement implies for the logarithmic derivative $|\Psi'/\Psi| \approx 1/\Delta$. This is an obvious geometrical fact, but in more physical terms it is a consequence of the uncertainty principle. Together with the matching condition between the logarithmic derivatives of the free motion wavefunction and of the wavefunction in the annihilation region $|\Psi'/\Psi|_{r=R_{nucleus}+\Delta} = |k \cdot \cotg\{k(R_{nucleus} + \Delta - \alpha)\}|$ this leads to the previous α -values in the limit $k \rightarrow 0$.

These values of course are deduced from approximate equations, so they represent just estimates, however they suggest that the antineutron annihilation cross sections should not show a *systematic* increase with the target mass number A . Such an increase could be present for antiproton annihilations, but because of Coulomb effects only. When going to any specific target nucleus, non-systematic effects could be present, especially related with the structure of the nuclear surface. An example is given in ref.[56]. There, anomalous behaviors are related with the non-sphericity of the nucleus. Another exception should be represented by neutron-halo nuclei, because in this case the annihilation range could be much larger than 1 fm. Also the composition of the nuclear surface in terms of protons or neutrons could be important, since all models attribute a strong isospin dependence to the antinucleon-nucleon interaction.

The exposed mechanism has an interesting consequence in the case of optical potential analyses: an increase of the strength of the imaginary part of the optical potential can lead to a decrease of the consequent reaction rate at small momenta[13,15–18]. In the above language, an increase in the potential strength leads to a decrease in the size parameter Δ , since the absorption of the projectile wavefunction takes place in a shorter range. Also modification of other parameters (radius, diffuseness, etc) leads to consequences that are not necessarily the most obvious ones. An example is given in the next section.

4 Comparison between $n\bar{p}$ and $\bar{p}p$ total annihilation cross sections.

In fig. 1 we show the TNA and TPA on Hydrogen, together with two fits by energy-independent optical potentials. For the $\bar{p}p$ case the total interaction in-

cludes the electrostatic potential of a spherical charge distribution with radius 1.25 fm. This charge radius is $\sqrt{2}$ times the charge radius of the proton, to take into account both the proton and the antiproton extended charges. Details on the potential are given below. A third optical potential curve shows what would be the $\bar{p}p$ cross section in absence of electrostatic interactions, within the same optical model.

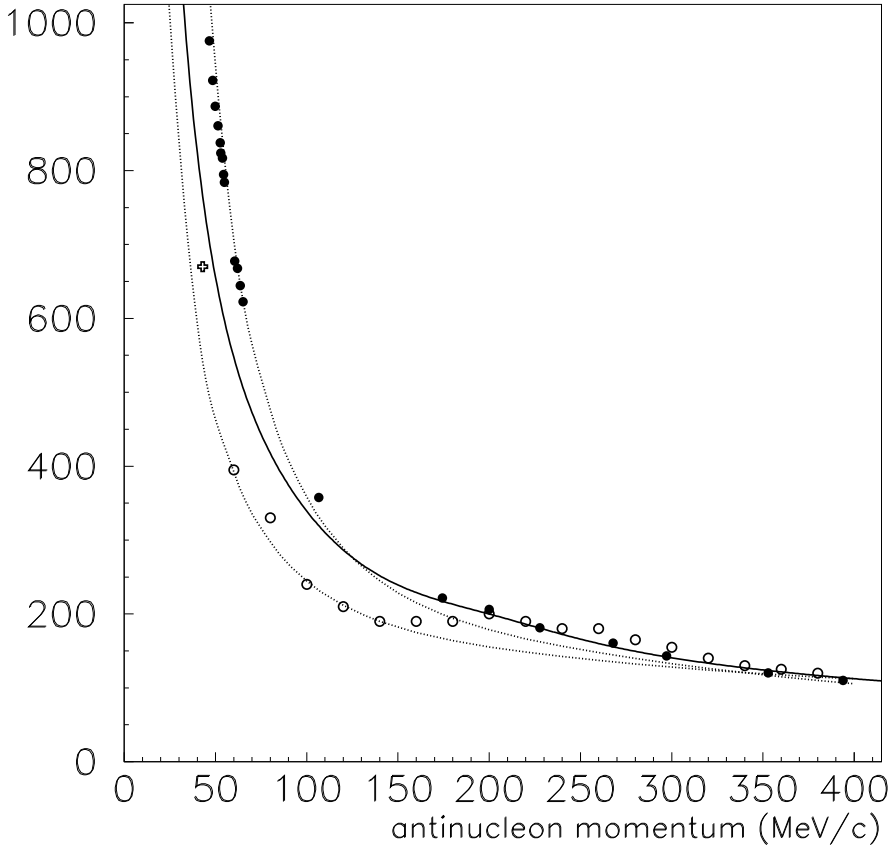


Fig. 1. Antineutron (empty circles) and antiproton (full circles) total annihilation cross sections (mb) measured by the Obelix experiment[1,3,4] (called TNA and TPA, respectively, in the text). The empty crosses reproduce the two low-energy $\bar{n}p$ total annihilation points measured in [57]. Error bars are not reported. The two dotted lines correspond to optical potential fits (see text for details). The solid line represents the $\bar{p}p$ annihilation cross section after Coulomb effects have been subtracted, as described in the text. The lower energy part of this curve has been calculated by extrapolating the optical potential fit of the $\bar{p}p$ data and by removing the electrostatic part of the potential. For $k > 30$ MeV/c the Coulomb effects have been subtracted from the actual $\bar{p}p$ points, not from the potential fit (for this reason the solid curve is larger than the dotted curve for $k > 130$ MeV/c).

What we notice first is that TNA and TPA are reasonably similar for $k > 200$ MeV/c, but below 200 MeV/c the TNA falls clearly below the TPA, and this

fall can not be justified in terms of Coulomb interactions only, although these contribute. We could speak of “low energy fall” with respect to a “background” which is similar to the $\bar{p}p$ case. Alternatively one can think that the TNA sums two contributions: a monotonous background that is proportional to the $\bar{p}p$ annihilation rate (Coulomb effects apart) but lower, and a broad peak (resonance?) at $k \sim 200\text{--}300$ MeV/c. This broad peak would be hidden by the isospin-0 background and by the low energy Coulomb rise in the TPA case. Some of the available data at momenta > 400 MeV/c (see [7] for a more systematic review of these data) could support the “peak” idea, since at these momenta the $\bar{n}p$ annihilation rate seems to be lower than the $\bar{p}p$ one, but it is not unequivocally clear how much lower. Indeed, one $\bar{n}p$ point at 700 MeV/c by [58] is clearly below the $\bar{p}p$ annihilation, while data reported in [59] are not very different from the corresponding $\bar{p}p$ data[60] in the region 300-500 MeV/c. On the other side, some data at very low energy[57] support the “gap” idea, since they show a rise of the $\bar{n}p$ annihilation rate $\beta\sigma$ below 50 MeV/c. These data have been reported in the figure, and the one at 20 MeV/c lies on the optical potential extrapolation of the $\bar{p}p$ data, once the electrostatic part of the potential has been removed. The authors of ref.[57] also report some potential predictions[41,43] that support the existence of a minimum for the $\bar{n}p$ annihilation rate $\beta\sigma_{ann}$ at 50-100 MeV/c, and a set of scattering length predictions[41,43,40] that show no great differences between $\bar{p}p$ and $\bar{n}p$ expected scattering lengths. They also report a collection of pre-Obelix \bar{n} data.

We must remark that the normalization of antineutron fluxes is a delicate matter, with the consequence that both a comparison of antineutron data coming from different experiments, and a comparison of antineutron and antiproton data, must be taken with the greatest caution. So we will generically speak of a “gap/peak structure” of the $\bar{n}p$ annihilation rate compared to the $\bar{p}p$ one. We will show in the next section that a comparison with nuclear data supports the existence of this gap/peak structure. Whatever the interpretation, there are some important remarks:

- 1) The strong oscillation of the TNA with respect to the TPA (see also fig.4) is an evidence of the fact that different physical mechanisms are dominating in the two cases in the considered momentum range. If a resonance is present this is obvious. If there is no resonance, according to the partial wave analyses presented in refs.[1,61] the TNA P-wave has its maximum at $k \approx 250$ MeV/c where it attains the value 120-140 mb. Our optical potential fit (which seems good for the TPA) fixes the TPA P-wave maximum to about 80 mb at 150 MeV/c. Semiclassical intuition fixes the corresponding impact parameters $b = L/k$ to 1.25 fm (TPA) and 0.8 fm (TNA). Then, purely geometrical considerations suggest a ratio, between the size of the two P-wave outcomes at their peak momentum, $\text{TNA}/\text{TPA} \sim (0.8/1.25)^2 \approx 0.4$ instead of the found value 1.6. The most obvious conclusion would be that the P-wave interaction is much more effective in the $\bar{n}p$ case, where it acts at smaller impact param-

eters (by a factor 0.6). This short range interaction does not affect the S-wave contribution, which is clearly larger in the $\bar{p}p$ case (even after subtracting Coulomb effects) at momenta over 30 MeV/c. At lower momenta (that means longer range) the two S-wave contributions could be equal, according to[57] and references therein. So the geometry and strength of the isospin-1 and isospin-0 channel interactions must be different, as far as these semiclassical considerations can be trusted.

2) Absurd as it may sound, the fact that at small momenta TNA are sensibly smaller than TPA could mean that the interactions are stronger in the $\bar{n}p$ case than in the $\bar{p}p$ one. This can be immediately seen in the choice of the optical model parameters. We used a Woods-Saxon form, with all parameters, but one, equal for TPA and TNA. TPA: imaginary strength 8000 MeV, real strength 46 MeV (attractive), imaginary radius 0.52 fm, real radius 1.89 fm, real and imaginary diffuseness 0.15 fm. These values fall in the ranges used by previous authors to fit elastic data[62], and its imaginary part is pretty similar to other previously used optical potentials (e.g. the one of ref.[50]). Many other sets of parameters, and also different potential shapes, can lead to similar results for the available low-energy data. Starting from this peculiar set, to obtain the TNA curve it is sufficient to increase the imaginary radius to 0.75 fm. Alternatively, one can obtain the TNA curve by leaving the imaginary radius at 0.51 fm and increasing the imaginary strength to about 12000-16000 MeV. So, to get a smaller cross section we need a “stronger” potential. This “inversion” behavior is another manifestation of the general shadowing mechanism discussed in section 3. In an optical potential model at small k an increase, e.g., of the imaginary strength W produces an increase of the reaction cross section for small values of W only. After a certain threshold, further increases of W lead to a decrease of the reaction cross section[13,16–18,15]. At a qualitative level this can be explained by the uncertainty principle: an increase in the strength of the imaginary part of the potential decreases the thickness of that spherical shell, surrounding the proton/nucleus target, where annihilations are supposed to take place. This introduces larger gradients in the projectile wavefunction. These larger gradients imply a larger logarithmic derivative, and therefore a smaller (imaginary part of the) scattering length.

3) In the case of $\bar{p}p$ annihilations below 600 MeV/c many quite different choices of potential parameters can fit them[16–18] (including a pure imaginary potential) without introducing a dependence of the parameters on energy. All these fits share some common features. They reproduce the data very well below 150 MeV/c and above 300 MeV/c. The fits remain satisfactory up to 600 MeV/c. In the region 150-300 MeV/c the fits stay slightly below the data. Alternatively, it is possible to choose the parameters so as to reproduce the data from 150 to 600 MeV/c, while at lower momenta the fits are above the data. So, we could say that an energy independent optical potential can produce a “background” around which a slight oscillation is present (positive for k in

the range 150-300 MeV/c, or negative for $k < 150$ MeV/c). In the TNA case the situation is qualitatively the same, but the oscillation is much stronger and more evident. So it seems that an energy-independent optical potential fit can be well related with the isospin-0 channel, which seemingly consists of the “background” only. A background with the same shape is also present in the isospin-1 channel, but this channel also contains an oscillation that is not reproduced by our set of optical potentials. As already remarked, we have no means to establish the nature of this oscillation.

4) We have also tried to change our optical potential shape so as to produce resonances that fit the gap/peak structure which is seen in the $\bar{n}p$ annihilation. We can not exclude that more attempts can lead to a good reproduction of the data in fig.1 (in the described “inversion plus resonance” regime there is no predictable relation between the changes of the potential and the shape of the output, which makes such attempts rather frustrating). We have not been able to reproduce satisfactorily these data, and perhaps more sophisticated potentials are necessary. It was however easy to get shapes that *qualitatively* looked similar. We tried with two kinds of potential: (i) Woods-Saxon (with attractive elastic part) (ii) Woods-Saxon like the previous one, plus a repulsive elastic surface barrier of gaussian shape (of the kind $\exp[-(r - r_o)^2]$). In both cases to get a broad peak where it must be it was necessary to enlarge the range of the elastic part to 2.5-3 fm. This is probably due to the fact that, despite the smallness of the radius of the imaginary part, most of the annihilations take place at $r \approx 1$ fm. So only a much wider attractive well can produce metastable states, within such models. Perhaps in a more sophisticated potential model, where different spin channels are clearly separated, it is possible to get a resonance in a spin channel where annihilation is less effective, so without the need for such a long range for the potential. We think that these interesting data really demand for a higher level potential analysis.

5 Annihilation on nuclei. Shadowing in the charge ratio.

Because of the shadowing, a complete analysis of annihilations in nuclei below 60 MeV/c is pretty complicated. A simple comparison of different sets of data reveals interesting features, however, and we can also hope to understand something by a PWIA analysis, especially at momenta over 100 MeV/c. In particular, the energy dependences of the $\bar{n}p$ annihilation cross section, of the \bar{n} -nucleus one, and of the ratio of $\bar{p}n$ to the $\bar{p}p$ annihilation in nuclei, show evident correlations. Of course nuclear shadowing effects are completely absent in PWIA, and this must be taken into account, taking with great care the calculations below 100 MeV/c. At larger momenta the main missed effect is the eclipse effect[38] which implies an almost energy independent surface absorption factor ≈ 0.5 . We take this factor into account by renormalizing our

PWIA predictions with one datum at a specified momentum value over 200 MeV/c.

At small momenta however (below ~ 200 MeV/c) shadowing is something more complicated than a mere eclipse effect. The eclipse effect could never bring \bar{p} annihilation rates to decrease with increasing A . So we may only *define* as “shadowing” the departures from PWIA predictions, and remark that they are consistent. As we show later, anyway, a certain part of the smallness of the low energy \bar{p} -Deuteron annihilation rate with respect to the $\bar{p}p$ one is not a shadowing effect, but just due to the smallness of the $\bar{p}n$ annihilation rate below 150 MeV/c.

In fig.2 we show the \bar{n} -nucleus data, relative to momenta between 180 and 280 MeV/c, for several nuclear species from ^{12}C to ^{207}Pb (see [2] for more details). These data are consistent with an $A^{2/3}$ law, expressing dominant surface absorption, *among them*. However the $A^{2/3}$ law found in these data cannot be generalized to $\bar{n}p$ or $\bar{p}p$ (Coulomb subtracted) data in the laboratory frame, while this generalization is only approximately possible in the center of mass frame. At 180 MeV/c, the ^{12}C or the ^{207}Pb TNA, divided by $A^{2/3}$, give about 150 mb. The corresponding $\bar{n}p$ and (Coulomb subtracted) $\bar{p}p$ cross sections are ≈ 200 mb at the same laboratory momentum. At the same center of mass momentum, which corresponds to 360 MeV/c in the laboratory, the $\bar{n}p$ total annihilation cross section is about 130 mb, and the $\bar{p}p$ one is slightly smaller than the $\bar{n}p$ one. So, in both cases we find deviations from the $A^{2/3}$ law at $k_{cm} \approx 100$ MeV/c, but these deviations are of opposite sign if the data are compared at the same laboratory or center of mass momentum. It is difficult to establish whether it is more proper to compare data relative to different nuclear species at the same laboratory or center of mass momentum. Impulse approximation based models suggest the same laboratory momentum, compound nucleus inspired models prefer the opposite choice. Indeed, in the former case direct momentum exchange is between the projectile and one of the target nucleons only, whose average initial momentum is zero in the laboratory. In the latter, the projectile momentum is given directly to the entire target nucleus.

An analogous, systematic comparison of all the available \bar{p} -nucleus data has been presented elsewhere[6].

Very recently a new series of \bar{n} -nucleus data down to 70 MeV/c has been presented[63], which show a respected $A^{2/3}$ law between different nuclear species. Since these data have been presented as “preliminary”, we can’t discuss them in detail.

Considering the energy behavior of the TNA on nuclei shown in fig.2, the most interesting feature is the systematic presence of a shoulder. However

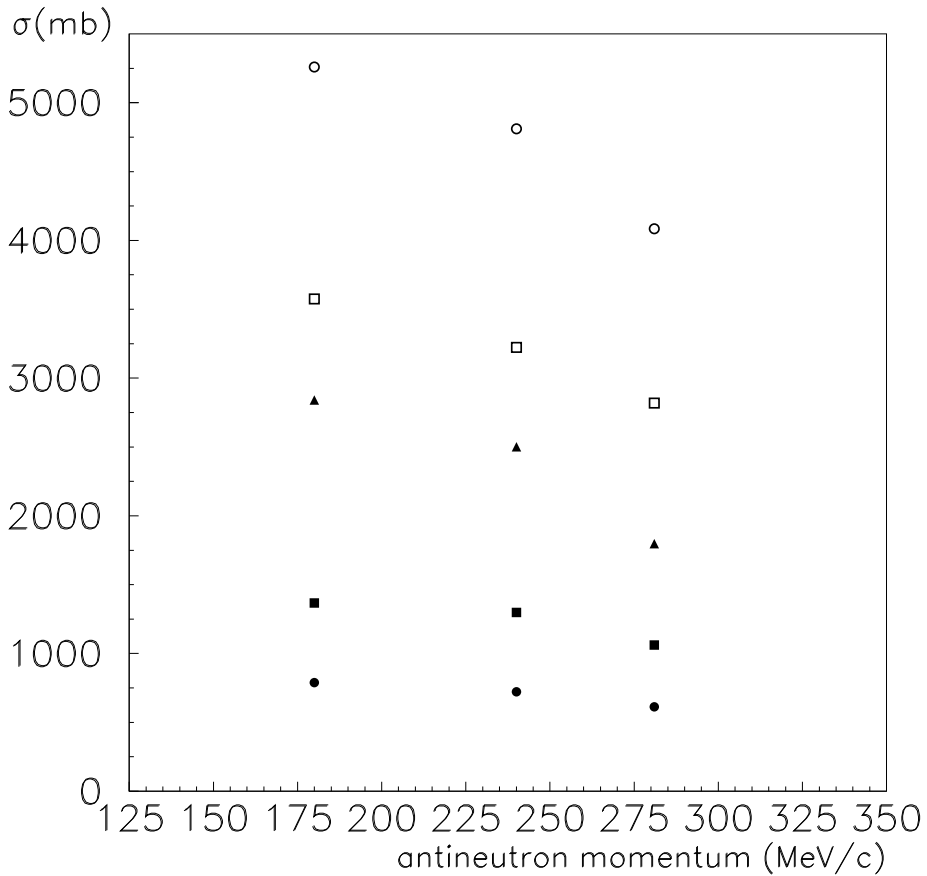


Fig. 2. \bar{n} -nucleus total annihilation cross sections for C (full circles), Al (full squares), Cu (full triangles), Sn (empty squares), Pb (empty circles). All the data have been taken at antineutron momenta 180, 240 and 281 MeV/c in the laboratory (see [2] for more details).

this phenomenon seems less evident in the just quoted preliminary data. TPA data in this region are not enough to give us shape information. However, the optical potential calculations that we have reported in [17] suggest that the Coulomb enhancement at low energies can easily hide such details in the energy dependence of the annihilation data.

Different relevant mechanisms must be taken into account in the momentum range 100-300 MeV/c:

- 1) The tail of the low energy shadowing phenomenon. Presently we have no knowledge of TPA and TNA on heavy nuclei at $k \ll 100$ MeV/c, so we do not know whether the discussed shadowing is a systematic phenomenon (as we suggest in the previous section 2) or is simply peculiar of some light nucleus. And in light nuclei we do not have enough TPA data in the region 100-300 MeV/c to understand completely the transition between large and

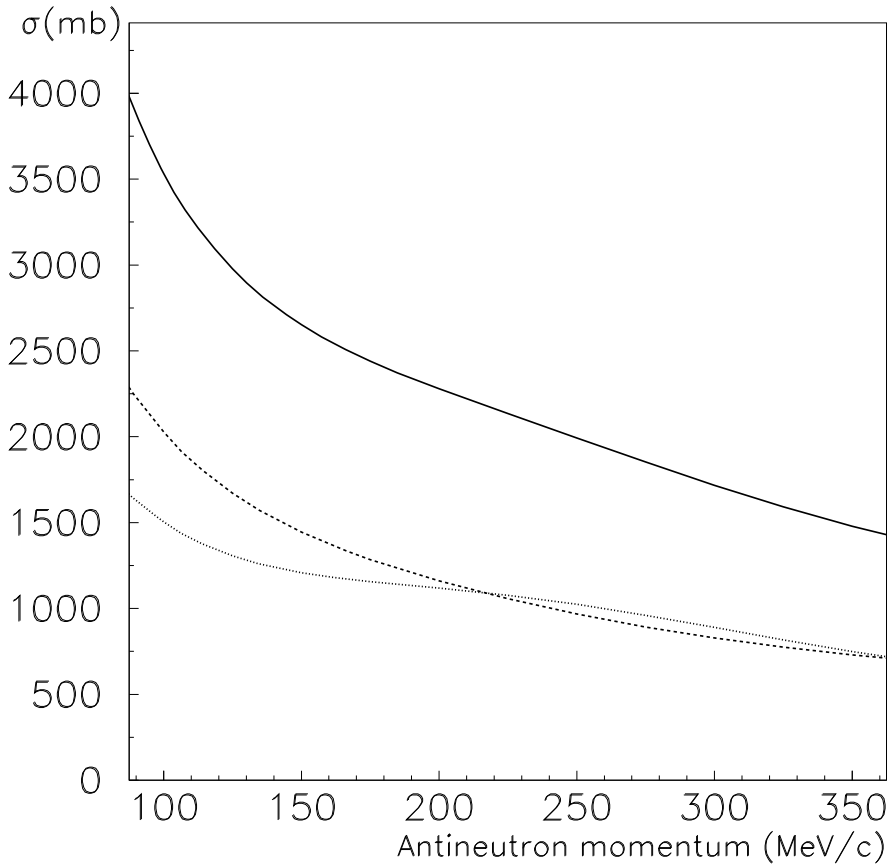


Fig. 3. PWIA calculation of the annihilation cross section $\bar{n}-{}^{40}Ca$. The reported curves have been multiplied by 0.5 to take absorption into account. This (approximate) factor has been estimated from the data in fig.2. Continuous curve: the total annihilation cross section. Dashed line: contribution from the $\bar{n}n$ annihilations. Dotted line: contribution from the $\bar{n}p$ annihilations.

low energy regimes. There are several sets of data, but regrettfully we do not have a satisfactorily continuous set of data relative to the same projectile on the same target (with the exception of the $\bar{p}p$ and $\bar{n}p$ cases).

3) The nuclear Fermi motion. The Fermi momentum, which represents a rough cutoff of the nuclear momentum distribution, is ≈ 200 MeV/c. This means that for $k < 200$ MeV/c the statistical distribution of the relative \bar{n} -nucleon motion contains the zero-energy point, and that it is easy for a target nucleon to be faster than the projectile. So the projectile momentum 200 MeV/c represents a kind of special borderline in the physics of annihilations on nuclei.

4) The $\bar{n}p$ annihilation cross section presents the above discussed gap/peak structure below 300 MeV/c. The nuclear Fermi motion will soften this structure, but perhaps not enough to make it completely disappear.

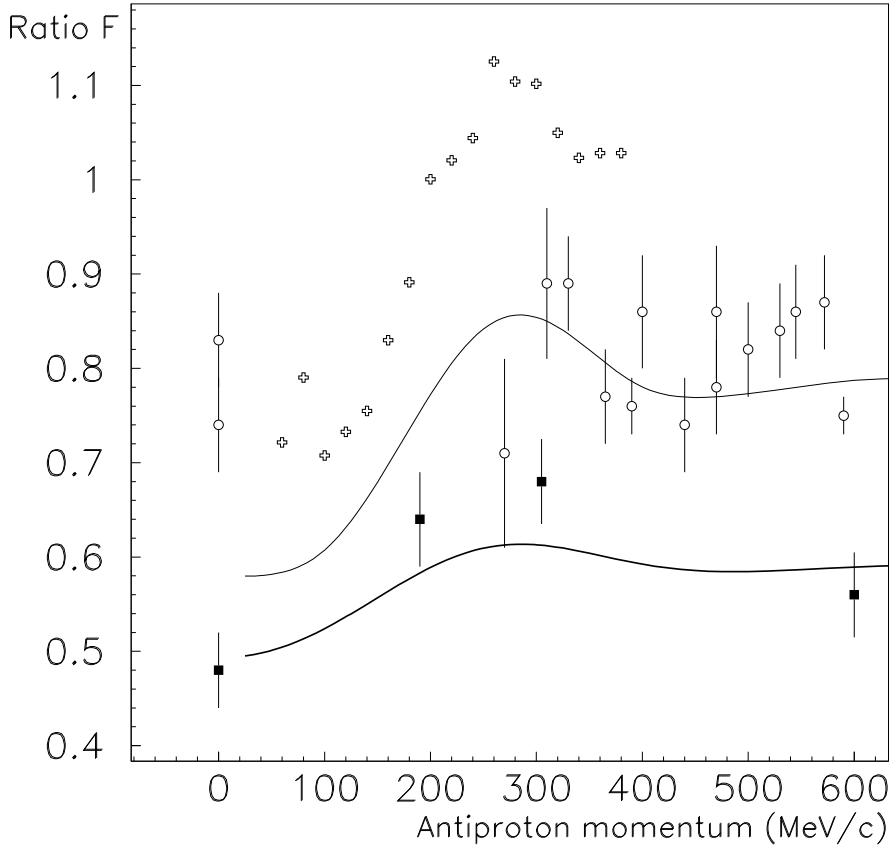


Fig. 4. Ratios F_A of antiproton annihilations on neutrons to antiproton annihilations on protons in a nucleus, for $A = 2$ (Deuteron - empty circles) and 4 (${}^4\text{He}$ - full squares). For more details about these data see [8]. The empty crosses represent, for comparison, the ratio F_1 between the $\bar{n}p$ total annihilation cross sections reported in [1] and the “Coulomb subtracted” $\bar{p}p$ total annihilation cross sections (continuous line in fig.1). The two continuous lines represent PWIA fits of F_2 and F_4 . To produce these fits the $\bar{n}p$ annihilation rates have been rescaled by an energy-independent factor α_A . For Deuteron $\alpha_2 = 0.8$, and for ${}^4\text{He}$ $\alpha_4 = 0.6$. More details on these PWIA fits are in the text.

A PWIA calculation can give some qualitative understanding about the roles of the gap/peak structure and of the Fermi motion in the nuclear TNA, and also about the relative role of neutrons and protons in the target.

In fig.3 we present a PWIA calculation of the TNA on ${}^{40}\text{Ca}$. In fig.4 we show a PWIA calculation of the F_A ratio on Deuteron and ${}^4\text{He}$. We recall that we have defined F_A as the ratio between \bar{p} annihilations on neutrons and protons inside a nucleus with mass number A . In figs. 5 and 6 we show PWIA calculations of \bar{p} annihilations on deuteron and ${}^4\text{He}$.

As a starting point we have used an equation contained in [16]. Although this

equation has been justified there by a long series of mathematical passages, its meaning is quite simple and can stand without demonstration: at PWIA level, any event rate on a nuclear target, leading to a well defined final state, is an incoherent sum of the rates of all the possible $\bar{n}n$ and $\bar{n}p$ events leading to the same final state, weighted by the nuclear momentum distribution of the target nucleon. By “rate” we mean a cross section divided by the corresponding flux of colliding particles. Under the simplifying assumption that different final states sum incoherently we simply have:

$$\beta(k, 0)\sigma(k) = \int N(\vec{k}')\beta(\vec{k}, \vec{k}')\sigma(|\vec{k} - \vec{k}'|)d^3k', \quad (1)$$

where $\beta(\vec{k}, \vec{k}')$ is the relative velocity between two colliding particles with momenta \vec{k} and \vec{k}' .

This nuclear PWIA average of the antinucleon-nucleon processes clearly misses any eclipse or shadowing effect (which, e.g., produces a TNA proportional to $A^{2/3}$ at large energies). So, the rise of the PWIA curve in fig.3 below 150 MeV/c is unreliable (it is just proportional to the average rise of antiproton and antineutron annihilation cross sections on a proton). At momenta larger than 150 MeV/c the PWIA should be more reliable, apart for a slowly energy dependent eclipse factor, and could clarify the effects of the Fermi motion and the different role of protons and neutrons in the target.

For the ^{40}Ca shells we have used harmonic oscillator eigenfunctions. Some attempts with different kinds of states have shown no qualitative differences, unless the nuclear size is changed to unphysical values. In addition, the most external wavefunctions do not show great differences (in the energy dependence of the outcome) with respect to the S-wave ground state. This is important, because in a more proper DWIA (distorted wave impulse approximation) treatment the internal shells would be scarcely involved in the annihilation process. For Deuteron and ^4He (in fig.4) experimental single particle momentum distributions[64] have been used. Again, within this simple model we did not find a great sensitivity of the results on the peculiarities of the momentum distribution, taking into account that many details that could be present in the numerator and in the denominator are lost in the ratios of fig.4. With Deuteron, we surely missed the angular dependence of the large momentum (D-wave dominated) part of the distribution.

To calculate the PWIA curves of figure 3 we need $\bar{n}p$ and $\bar{n}n$ annihilation rates. For fig.4 we need $\bar{p}p$ and $\bar{p}n$ annihilation rates, both subject to the effect of the Deuteron or ^4He charge. The $\bar{n}n$ annihilation rate has been assumed to be equal to the Coulomb subtracted $\bar{p}p$ one (i.e. the continuous curve of fig.1). In fig.4 we use the same cross sections, so we neglect the effects of the nuclear electrostatic attraction. On the basis of the discussion in section 2 we assume

that they do not affect the F_A ratio, although they surely enhance both the $\bar{p}p_{in\ nucleus}$ and the $\bar{p}n_{in\ nucleus}$ rates. Actually a look at the data in fig.4 shows that (with large error bars) $F_4/F_2 \simeq 0.48/0.78 \simeq 0.61$ at zero energy, and $0.54/0.82 \simeq 0.66$ at about 600 MeV/c. In the case of a different action of the nuclear electrostatic potential on the $\bar{p}p$ and $\bar{p}n$ cross sections, this effect would be practically absent at 600 MeV/c and would depress the F_4 ratio with respect to the F_2 one at momenta $<< 100$ MeV/c. The large error bars and data fluctuations do not allow for easy conclusions, however there are no special reasons to assume a different Coulomb effect on $\bar{p}p$ and $\bar{p}n$ reactions, if both the proton and the neutron are bound in the same nucleus.

The Obelix $\bar{n}p$ data cover the range 60-400 MeV/c, and the $\bar{p}p$ ones start at 30 MeV/c. We therefore had to assume values for these cross sections for momenta outside these ranges. With $\bar{p}p$ data at momenta over 200 MeV/c we have relied on the data in ref.[60], and at momenta below 30 MeV/c on our optical potential fit (after subtraction of Coulomb forces as in fig.1). For the $\bar{n}p$ case, in the region $k > 400$ MeV/c the $\bar{n}p$ data have been assumed to be equal to the $\bar{p}p$ ones, as suggested by the measurements in ref.[59] and [60] for momenta over 300 MeV/c (see e.g. [7], fig.9, for a comparison of the $\bar{n}p$ and $\bar{p}p$ data in that momentum range). A look at fig.4 does not help too much. Indeed, we may say that the nuclear Fermi motion approximately averages the “free” annihilation rates within a 200 MeV/c range. Then the point of view of equal “free” $\bar{p}p$ and $\bar{p}n$ annihilation rates at momenta in the range 300-600 MeV/c can be supported by the absence of a clear decreasing trend in the set of Deuteron points over 300 MeV/c. On the contrary, the Helium point at 600 MeV/c supports the possibility of a decrease of the free $\bar{p}n/\bar{p}p$ ratio, as suggested by the measurement in ref.[58]. Anyway, the scatter of data in the deuteron case, and the lack of data in the ^4He case prevent us from precise conclusions. In the limit of zero energy, we have adopted the low energy parametrization of the $\bar{n}p$ cross section contained in references[1,61]. It implies a decrease of the F_A ratios at very low energies, which is more suitable for fitting the zero-energy ^4He point. Adopting the low energy parameters suggested by refs.[57,40,41,43] would on the contrary rise the zero energy F_A value, which is more coherent with the two zero-energy Deuteron points.

The upper curve in fig.3 can be taken as a qualitative confirmation of the effect of the $\bar{n}p$ gap/peak structure in producing a very soft shoulder in the \bar{n} -nucleus annihilations at 150-300 MeV/c. In fig.3 we also show the separate contributions of the $\bar{n}p$ and $\bar{n}n$ reactions. Evidently the $\bar{n}n$ reaction alone would not interrupt the trend of a positive second derivative that characterizes expectation and data at both lower and larger momenta. Within PWIA the shoulder is a direct consequence of the gap/peak structure of the $\bar{n}p$ cross section. The Fermi motion, as predictable, softens this gap/peak structure, but not completely. We must also observe that the produced shoulder is much less pronounced than most of the ones seen in fig.2. Our attempts with different

shapes for the nuclear shells show that the shoulder evidence is enhanced by a larger radius of each nuclear shell (i.e. a narrower momentum distribution), however one must arrive at slightly unrealistic nuclear dimensions in order to obtain more evident shoulders.

The strength of the rise of the PWIA cross sections below 100 MeV/c is probably unphysical, since we know that shadowing could be very active in that region (although the quoted recent preliminary data [63] confine shadowing to $k < 70$ MeV/c and with good approximation reproduce the predictions of fig.3). In ref.[17] some optical potential shapes possibly corresponding to low energy \bar{n} -nucleus annihilations are reported, and they are almost energy-independent in the region 100-300 MeV/c. These optical potentials were based on Coulomb-subtracted $\bar{p}p$ data and on nuclear cross sections at momenta over 200 MeV/c and so have no relation with that gap/peak structure that is peculiar of the $\bar{n}p$ interaction. The data reported in [63] confirm the IA behavior reported in fig.3 down to 70 MeV/c, rather than the these optical potential predictions.

The systematic presence of the gap/peak structure in the TNA/TPA ratio is much more evident in fig.4, where we report the F_A ratio for $A = 1$ ($\bar{n}p$ data coming from the Obelix experiment[1] divided by the Coulomb subtracted $\bar{p}p$ annihilation cross section represented by the continuous line in fig.1), for $A = 2$ (Deuteron) and $A = 4$ (^4He). These Deuteron and ^4He data come from several experiments and are reviewed in ref.[8].

Looking at fig.4 one immediately notices that all deuteron points lie above any of the ^4He points, and the proton target data are, in the average, clearly over the nuclear target data (we remark that, although the proton target ratios have been calculated using the “Coulomb subtracted” $\bar{p}p$ annihilation cross section, the effect of the Coulomb subtraction is negligible above 100 MeV/c). The second observation concerning the data reported in fig.4 is that a certain degree of correlation between the shapes of the three groups of data is present.

Since $Z/A = 1$ both in Deuteron and ^4He , and the average value of the free F_1 ratio is about 1, clearly PWIA cannot reproduce the average value of these nuclear F_A distributions. For producing the fits contained in fig.3 we have multiplied the $\bar{n}p$ total annihilation cross section by a constant factor α , which is 0.8 for Deuteron target, and 0.6 for ^4He target. At the largest energies of the considered range the PWIA ratio should be reliable. The known eclipse effect should more or less cancel between numerator and denominator. Anomalous shadowing of the kind discussed in section 3 is not strong over 100 MeV/c. So the reason for $\alpha_{^4\text{He}} < \alpha_D < \alpha_p \equiv 1$ is unexplained. A possibility is final state rescattering. This should not be very effective in total annihilation cross sections, but in the F_A case it can modify the number of charged particles that is used to decide whether the annihilation was on a proton or on a neutron.

It is not unlikely that this A -dependent renormalization effect has this origin, however one should analyze carefully how each experimental point has been measured.

In the case of ${}^4\text{He}$ the PWIA fit reproduces satisfactorily the behavior of the data. We may say that the gap/peak structure of the free $\bar{n}p/\bar{p}p$ ratio is reproduced by the F_4 ratio. In the Deuteron case at zero-energy the fit is not satisfactory, while over 200 MeV/c some correlation seems to be present. Somehow the presence of the PWIA peak at 280 MeV/c (which is a consequence of the gap/peak structure of the free ratio) is reflected in the presence of a maximum in the data at 300 MeV/c, but the large error bars and the spread of the data do not allow for more quantitative conclusions.

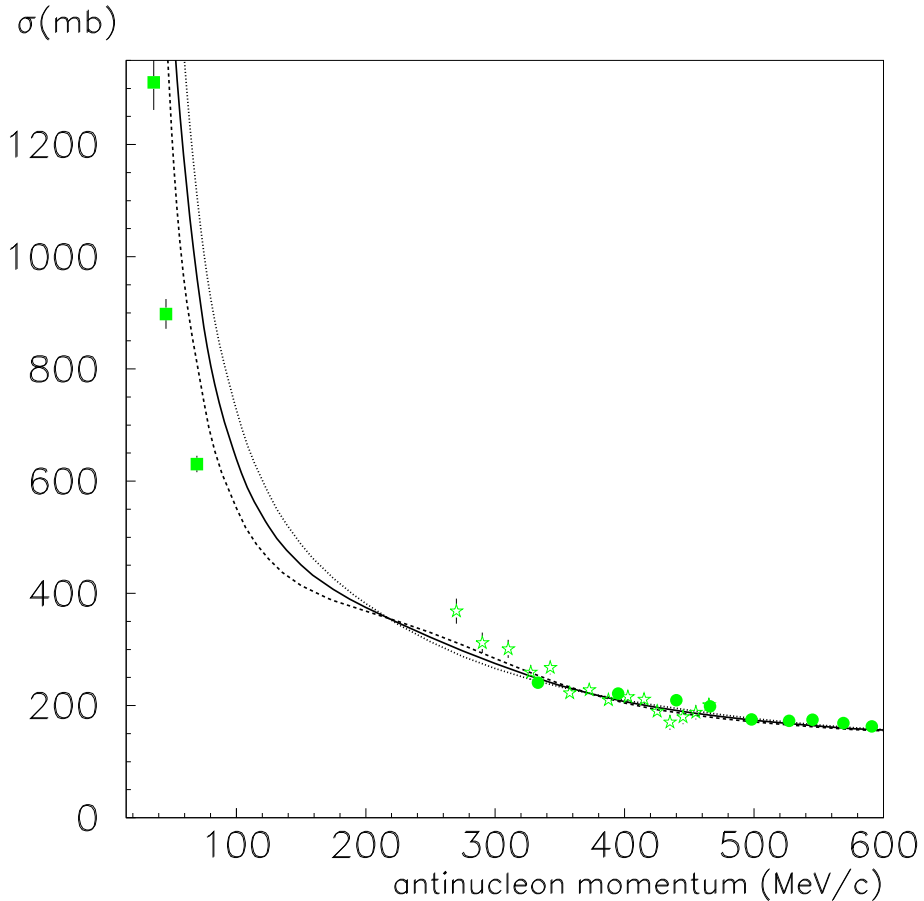


Fig. 5. PWIA calculation of the \bar{p} -Deuteron total annihilation cross sections, together with data points taken from references [5] (full squares), [65] (empty stars), [66] (full circles). Continuous line: full PWIA calculation with Coulomb correction and renormalization of the curve to the point at 340 MeV/c. Dashed line: the Deuteron is supposed to be composed by two neutrons (with overall nuclear charge $Z=1$). Dotted line: the Deuteron is supposed to be composed by two protons (with overall nuclear charge $Z=1$). See the text for more details.

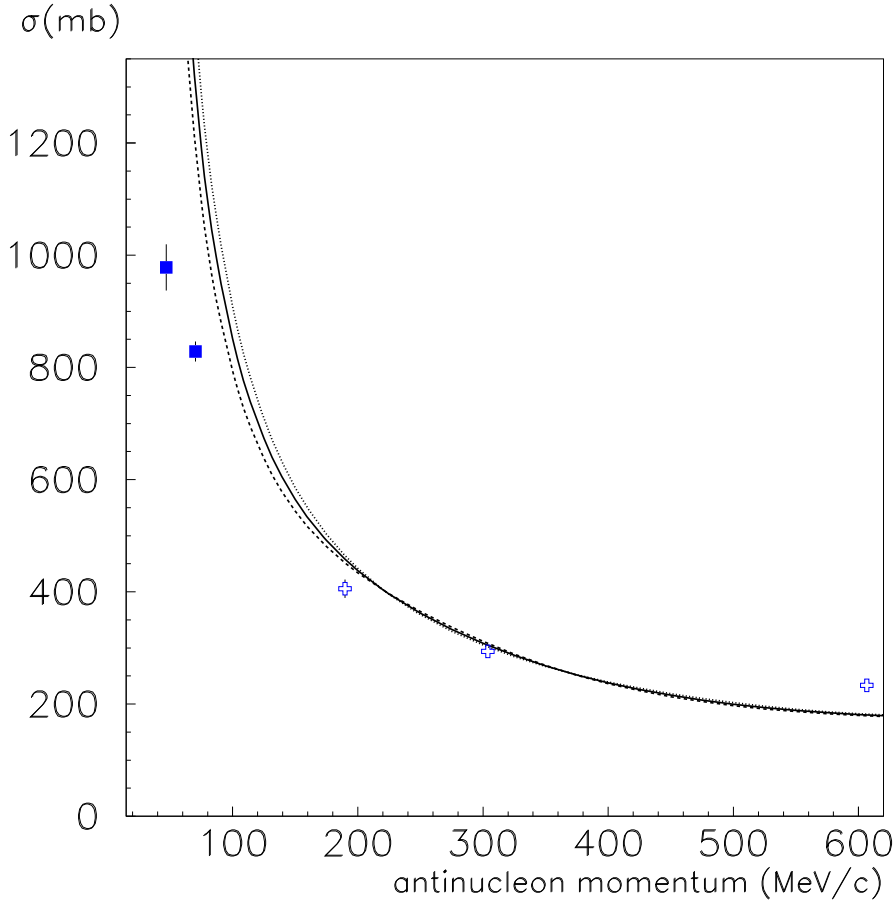


Fig. 6. PWIA calculation of the \bar{p} - ${}^4\text{He}$ total annihilation cross sections, together with data points taken from references [5] (full squares), [67] (empty crosses). Continuous line: full PWIA calculation with Coulomb correction and renormalization of the curve to the point at 300 MeV/c. Dashed line: the nucleus is supposed to be composed by four neutrons (with overall nuclear charge $Z=2$). Dotted line: the Deuteron is supposed to be composed by four protons (with overall nuclear charge $Z=2$). See the text for more details.

In the last two figures we show some PWIA fits of the \bar{p} annihilation cross sections on Deuteron and ${}^4\text{He}$. To obtain these curves the same above method has been used, but the final result has been multiplied, to take the nuclear charge into account in agreement with ref.[17], by the factor $1+ZC\beta^{-1.4}$, where Z is the nuclear charge, β is the \bar{p} -nucleus relative velocity and the constant C is characteristic of the target nucleus. The exponent (-1.4) has no special physical meaning, since the above $1+ZC\beta^{-1.4}$ factor is only a fitting relation that reproduces within some percent the Coulomb enhancement factor in the range 40-400 MeV/c. The constant C is 0.0060 for Deuteron, and 0.0040 for ${}^4\text{He}$. To take surface absorption into account, the two PWIA fits have been renormalized by a constant factor, the best to reproduce the data (or some data) over 200 MeV/c. We remark that: (i) this Coulomb factor is not relevant

from 100 MeV/c onward, (ii) it is not very different between light nuclei at the same \bar{p} momentum in the laboratory frame, (iii) in Hydrogen, Deuteron and ^4He it is near 1.5 at 50 MeV/c and 2 at 25 MeV/c (laboratory frame).

In the two figures we also report what would be the PWIA distribution if the target nucleus were composed by neutrons only or by protons only (without touching the Deuteron and ^4He charges, which are taken into account by the $1+ZC\beta^{-1.4}$ factor in any case). The first evident observation is that the effect of the $\bar{n}p$ gap/peak structure is much more evident in the Deuteron case. This is due to the compactness of the ^4He structure, and to the exactly opposite peculiarity of the Deuteron structure. A more compact space structure implies a broader momentum distribution. The Fermi motion tends to average out the details of the momentum dependence of the nucleon-antinucleon annihilation rates. This mechanism is more effective with broader nuclear momentum distributions. Another observation is that, if we define shadowing as the departure between the observed data and Impulse Approximation predictions, this departure becomes evident in both cases below 100 MeV/c, but more evident in the ^4He case. In the Deuteron case the shadowing phenomenon is less dramatic, but would be overestimated by not taking into account that one of the two nucleons composing this nucleus is a neutron.

Concluding this section, we may say that some evident correlation exists between nuclear data and the behavior of the $\bar{n}p$ annihilation rate. In particular, it would be difficult to justify the shape of the F_4 and F_2 ratios in absence of the gap/peak structure of the free $\bar{n}p/\bar{p}p$ ratio. There is some chance that the shoulder found in the \bar{n} -nucleus annihilation cross sections is related with the same gap/peak structure, however in this case the situation is much less clear. Still to be clarified is the fact that the energy-averaged value of the F_A ratio decreases at increasing A . The last two figures also show that the energy dependence of the nuclear annihilation rates can be partly explained in terms of the energy dependence of the \bar{p} annihilation cross section on a free neutron. A consistent part of this energy dependence, however, cannot be explained in these terms and we may say that a strong energy-dependent shadowing is present.

6 Conclusions.

We have presented an analysis comparing low energy $\bar{n}p$ annihilation data with other available data on antinucleon-nucleon and antinucleon-nucleus annihilation. The different sets are all consistent with a gap/peak structure in the isospin-1 channel, over a regular “background” which can be reproduced by energy-independent optical potentials of simple form. This structure is not too pronounced but evident, and we have also shown that it affects the nu-

clear annihilation rates, whose behavior can be *partly* explained in terms of the behavior of the antiproton-neutron annihilation rate.

We have also discussed the shadowing phenomena related with antinucleon-nucleus annihilation, and reported an interpretation in terms of the quantum uncertainty principle. The comparison of impulse approximation predictions with the nuclear data suggests that a strong energy-dependent shadowing is present at low energies: also after including absorption corrections, the data can not be fully explained in terms of individual antinucleon-nucleon annihilations.

References

- [1] A.Feliciello for the Obelix Collaboration, “Workshop on Hadron Spectroscopy 99”, March 8-12 1999, LNF Frascati (Italy), 429; M.Agnello *et al*, Nucl. Instr. Methods Phys. Res. A399 (1997) II; Nucl.Phys. **B** (Proc. Suppl.) 56 A (1997) 227.
- [2] V.G.Ableev *et al.*, Il Nuovo Cimento **107 A** (1994) 943
- [3] A. Zenoni *et al*, Phys. Lett. **B 461** (1999) 405.
- [4] A.Bertin *et al*, Phys. Lett. **B369** (1996) 77.
- [5] A. Zenoni *et al*, Phys. Lett. **B 461** (1999) 413.
- [6] A.Bianconi *et al*, in print on Phys. Lett. **B**.
- [7] G.Bendiscioli and D.Kharzeev, Rivista del Nuovo Cimento **17** (1994) 1
- [8] G.Bendiscioli, in “Antiproton-nucleon and antiproton-nucleus interactions”, eds. F.Bradamante, J.-M.Richard and R.Klapish, Ettore Majorana international science series, Plenum Press 1990, p.293.
- [9] A.Benedettini *et al*, Nucl. Phys. **B** (Proc. Suppl.) 56 A (1997) 58.
- [10] M.Augsburger *et al*, Phys. Lett. **B 461** (1999) 417.
- [11] S.Wycech, A.M.Green and J.A.Niskanen, Phys.Lett. **B 152** (1985), 308.
- [12] G.Q.Liu, J.M.Richard and S.Wycech, Phys.Lett **B260** (1991) 15.
- [13] K.V.Protasov, “Workshop on hadron spectroscopy 99”, March 8-12, 1999, LNF, Frascati (Italy), 463.
- [14] K.V.Protasov, G.Bonomi, E.Lodi Rizzini and A.Zenoni, in print on Eur.Phys.Jour. **A** (1999).
- [15] V.A.Karmanov, K.V.Protasov and A.Yu.Voronin, in print on Eur. Phys. Jour.

- [16] A.Bianconi, G.Bonomi, E.Lodi Rizzini, L.Venturelli and A.Zenoni, nucl-th/9910031.
- [17] A.Bianconi, G.Bonomi, E.Lodi Rizzini, L.Venturelli and A.Zenoni, nucl-th/9912025, in print on Phys. Rev. **C**.
- [18] A.Bianconi, G.Bonomi, M.P.Bussa, E.Lodi Rizzini, L.Venturelli and A.Zenoni, preprint nucl-th/0002015, in print on Phys. Lett. **B**.
- [19] A.Bianconi, G.Bonomi, M.P.Bussa, E.Lodi Rizzini, L.Venturelli and A.Zenoni, preprint nucl-th/0003006, submitted to Phys. Lett. **B**.
- [20] C.B.Dover, T.Gutsche, M.Maruyama and A.Faessler, Progr. Part. Nucl. Phys. **29** (1992) 87.
- [21] C.Amsler and F.Myhrer, Ann. Rev. Nucl. Part. Sci. **41** (1991) 219.
- [22] B.O.Kerbikov, L.A.Kondratyuk and M.G.Saposhnikov, Sov. Phys. Usp. **32** (1989) 739.
- [23] T.Walcher, Ann. Rev. Nucl. Part. Sci. **38** (1988) 1.
- [24] W.Weise, Nucl. Phys. **A558** (1993) 219c.
- [25] A review on the Compled channel model is given by I.S.Shapiro and a review on quark models by A.M.Green in “Antiproton-nucleon and antiproton-nucleus interactions”, eds. F.Bradamante, J.-M.Richard and R.Klapish, Ettore Majorana international science series, Plenum Press 1990, pg.81 and pg.109.
- [26] A.M.Green and J.A.Niskanen, International Review of Nuclear Physics, Vol.1, pg.570, World Scientific, 1984.
- [27] J.J. De Swart and R. Timmermans, “The Antibaryon - Baryon interactions”, Proceedings of the LEAP’94 Conference, World Sientific 1994, p.20.
- [28] C.J.Batty, in “Antiproton-nucleon and antiproton-nucleus interactions”, eds. F.Bradamante, J.-M.Richard and R.Klapish, Ettore Majorana international science series, Plenum Press 1990, p.251.
- [29] J.Eades and F.J.Hartmann, Rew. Mod. Phys. **71** (1999), 373.
- [30] C.J.Batty, Phys. Lett. **B 189** (1987) 393.
- [31] A.Deloff and J.Law, Phys. Rev. **C 10** (1974) 2657.
- [32] J.Thaler, J. Phys. G Nucl. Phys. **11** (1985) 689.
- [33] J.R.Rook, Nucl. Phys. **A 326** (1979) 244.
- [34] A.M.Green and J.A.Niskanen, Progr. Nucl. Part. Phys. **18** (1987) 93.
- [35] O.Dumbrais *et al*, Nucl. Phys. **A 457** (1987) 491.
- [36] A.K.Kerman, H.McManus and R.M.Thaler, Ann. Phys. **8** (1959) 551.

[37] A.S.Jensen, in “Antiproton-nucleon and antiproton-nucleus interactions”, eds. F.Bradamante, J.-M.Richard and R.Klapish, Ettore Majorana international science series, Plenum Press 1990, p.205.

[38] V.Franco and R.J. Glauber, *Phys.Rev.* **142** (1966) 1195.

[39] O.D.Dalkarov and V.A.Karmanov, *Sov. Journ. Nucl. Phys.* **45** (1987) 430; *Nucl. Phys. A* **478** (1988) 635c; G.Bendiscioli, A.Rotondi and A.Zenoni, *Nuovo Cim.* **104 A** (1991) 59.

[40] R.A.Bryan and R.J.Phillips, *Nucl. Phys. B* **5** (1968) 201, and **B 7** (1968) 481.

[41] C.B.Dover and J.M.Richard, *Phys. Rev. C* **21** (1980) 1466.

[42] J.M.Richard and M.E.Sainio, *Phys. Lett. B* **110** (1982) 349.

[43] J.Cote *et al*, *Phys. Rev. Lett.* **48** (1982) 1319.

[44] R.A.Freedman, W.Y.P.Hwang, and L.Wilets, *Phys.Rev. D* **23** (1981) 1103.

[45] M.A.Alberg *et al*, *Phys. Rev. D* **27** (1983) 536.

[46] M.Lacombe, B.Loiseau, B.Moussallam and R.Vinh Mau, *Phys. Lett. B* **124** (1983) 443.

[47] M.Mizutani, F.Myhrer and R.Tegen, *Phys. Rev. D* **32** (1985) 1163.

[48] F.Myhrer and R.Tegen *Phys. Lett. B* **162** (1985) 237.

[49] R.Tegen, F.Myhrer and T.Mizutani, *Phys. Lett. 182* (1986) 6.

[50] M.Kohno and W.Weise, *Nucl. Phys. A554* (1986) 429.

[51] J.Haidembauer, T.Hippchen, K.Holinde and J.Speth, *Z.Phys.A* **334** (1989), 467.

[52] E.g.: L.D.Landau and E.M.Lifshits: A course in theoretical physics, vol.III “quantum mechanics”.

[53] J.Carbonell and K.V.Protasov, *Hyp. Int.* **76** (1993) 327.

[54] J.Carbonell, K.V. Protasov and A.Zenoni, *Phys. Lett. B* **397** (1997) 345.

[55] W.Brückner *et al*, *Z.Phys. A* **339** (1991), 379.

[56] A.M.Green, G.Q.Liu and S.W.Wycech, *Nucl. Phys. A* **483** (1988) 619.

[57] G.S.Mutchler *et al*, *Phys. Rev. D* **38** (1988) 742.

[58] S.Banerjee *et al*, *Z. Phys. C* **28** (1985) 163.

[59] T.Armstrong *et al*, *Phys. Rev. D* **36** (3) (1987), 659

[60] W.Brückner *et al*, *Z. Phys. A* **335** (1990) 217.

[61] J.Mahalanabis, H.J.Pirner and T.A.Shibata, *Nucl. Phys. A485* (1988) 546.

- [62] W.Brückner *et al*, Phys. Lett. **B166** (1986) 113.
- [63] Data presented by E.Botta at the conference “Bologna 2000 - Structure of the nucleus at the dawn of the century”, may 29 - jun 3 2000, Bologna, Italy.
- [64] S.Frullani and J.Mougey, “Single particle properties of nuclei through (e,e’p) reactions”, Vol. 14 of Advances in nuclear physics, Plenum Press, New York - London; S. Boffi, C. Giusti and F. D. Pacati, Phys. Rep. **226**, 1 (1993); S.Boffi, C.Giusti, F.D.Pacati and M.Radici, ”Electromagnetic Response of Atomic Nuclei”, Vol. 20 of ”Oxford Studies in Nuclear Physics” (Oxford University Press, Oxford, 1996).
- [65] T.Kalogeropoulos and G.S.Tzanakos, Phys. Rev. **D 22** (1980) 2585.
- [66] R.Bizzarri *et al*, Il Nuovo Cimento **A** (1980) 225.
- [67] F.Balestra *et al*, Phys. Lett. **B 165** (1985) 265.